27th INTERNATIONAL CONGRESS OF MECHANICAL ENGENEERING
COBEM 2023
ABCM Brazilian Society of Mechanical Sciences and Engineering
27th ABCM International Congress of Mechanical Engineering
December 04-08, 2023, Florianópolis-SC, Brazil

COB-2023-2428
INTEGRATION OF FEM TO DETERMINE THE MICROSTRUCTURE AND FORMABILITY OF A CONTINUOUS COOLING BAINITIC STEEL

Thiago Marques Ivaniski
Antonio Carlos de Figueiredo Silveira
Metallurgy Department, Federal University of Rio Grande do Sul, Porto Alegre RS, Brazil, Leibniz Institut für Werkstofforientierte Technologien, Universität Bremen, Bremen, Germany.
thiago.ivaniski@ufrgs.br , silveira@iwt-bremen.de
Pedro José de Castro
Leibniz Institut für Werkstofforientierte Technologien, Universität Bremen, Bremen, Germany.
castro@iwt-bremen.de
Jérémy Epp
Leibniz Institut für Werkstofforientierte Technologien, Universität Bremen, Bremen, Germany.
epp@iwt-bremen.de
Alexandre da Silva Rocha
Metallurgy Department, Federal University of Rio Grande do Sul, Porto Alegre RS, Brazil
alexandre.rocha@ufrgs.br

Abstract. *The ongoing research endeavors are focused on advancing Continuous Cooling Bainitic Steels with the primary objective of mitigating manufacturing complexities and minimizing energy consumption within the forging industry. Nonetheless, a significant gap persists in the comprehension pertaining to their practical utilization. The control of stress state, plastic deformation, strain rate, and temperature directly impacts the workability of forged products. One approach that aims to enhance the understanding of the final mechanical properties of the forging is through the determination of dislocation densities during thermomechanical processing. The finite element simulation, once calibrated, allows observing these variations during hot forging. Therefore, this work aimed to determine dislocation density in austenite field of a wedge-shaped part during the forging step through the numerical simulation and compare it with the final dislocation density after the continuous cooling program. The findings indicate that, as the degree of plastic deformation in the austenite field increases, the dislocation density increases subsequent to the continuously cooled bainitic transformation, which is in direct correlation with the evolution of the microstructure during dynamic recrystallization and austenite grain refining.*

Keywords: *Hot Forging, Formability, Numerical Simulation, Microstructure, Dislocation density.*

1. INTRODUCTION

Forging stands as a prominent manufacturing process that holds substantial significance in the e.g., automotive, marine, and aerospace sectors. The scientific principles governing forging play a fundamental role in the production of automotive components characterized by exceptional fatigue strength and various other desirable properties.

Recently, the automotive industry is increasingly driven by reducing energy consumption during the production of components. To address this demand, an optimal solution lies in modifying the thermomechanical processing routes through the elimination of quenching and tempering (Q&T) subsequent to forging, moreover enhancing the tribological properties by surface engineering (Menezes, 2021; Dalcin et al., 2022).

During the continuous cooling process, the austenite undergoes a transformation into bainitic ferrite and there is still a debate about the nature of the transformation mechanism (displacive or diffusive). However, it will not be the object of matter in this report. In general agreement, the transformed microstructure is characterized by fine bainitic ferrite plates and retained austenite. The presence of retained austenite imparts a unique combination of strength and ductility that cannot be achieved with other microstructures (Bhadeshia, 1983; Sourmail, 2017).

It is well-established that the dislocation density plays a significant role in influencing the kinetics of transformation, exhibiting a direct correlation with the effects induced by diffusion during the nucleation and growth of new polycrystals in the forging process (Ivaniski et al., 2022; Hatwig et al., 2021). The relationship between dislocation density and various factors which occurs in hot forging such as strain, deformation temperature, and strain rate, can be established. In further development of the K-M model, Estrin and Mecking (Estrin and Mecking, 1984) introduced a comprehensive phenomenological framework to describe the dislocation density evolution during work hardening. In their study, Jonas et al., 2009, presented an advanced methodology for modeling the progression of dislocation density within grains undergoing exclusive dynamic recovery, employing flow curves derived from experimental data. The equation proposed by Quelennec et al. 2011 establishes a relationship for the mean dislocation density in grains experiencing dynamic discontinuous recrystallization (*dDRX*). The initiation of *dDRX* at the critical strain leads to an initial average dislocation density for recrystallized grains. By employing both the modeled dislocation density and the experimental dislocation density obtained from the flow curves, it is possible to determine the fraction of recrystallization attributed to dynamic recrystallization and express it using the Avrami equation (Avrami, 1939). By incorporating these models into finite element software, it becomes feasible to assess the dislocation density within the austenitic region relying on the plastic flow curves.

The objective of this preliminary investigation is to ascertain the dislocation density in the austenitic field during the forging of a wedge, utilizing finite element simulations, and subsequently compare it with the dislocation density data obtained from continuously cooled bainite. The aim is to establish a correlation between the extent of plastic deformation and the dislocation density arising from bainite.

2. METHODOLOGY

The utilized material in this study was DIN 18MnCrSiMo6-4 steel, specifically designed for continuous cooling, and classified as a carbide-free, low-carbon bainitic steel. A comprehensive overview of the complete metallurgical characterization and mathematical modeling methodology can be observed in Figure 1.

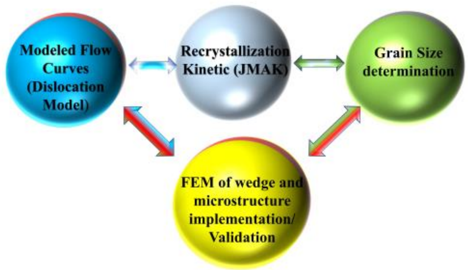

Figure 1. A schematic representation of the procedural steps involved in characterizing the rheological and metallurgical behavior for the purpose of calibrating finite element software is presented.

The software implemented flow curve models, governing the plastic behavior, were parameterized utilizing the Arrhenius equations, ultimately leading to the determination of the Zener-Hollomon equation specific to the material. To capture the physical behavior, the Estrin-Mecking approach (Estrin and Mecking, 1984) was employed to account for the dependency of dislocation density in the flow stress (Figure 2). This enabled the modeling of the material's plastic behavior at elevated strain rates and temperature levels that may not be feasible to achieve in laboratory-scale experiments. For a comprehensive elucidation of the methodologies employed in the rheological and metallurgical characterization of this bainitic steel, please refer to articles (Ivaniski et. al., 2020., Ivaniski et.al, 2022., Ivaniski et. al., 2022).

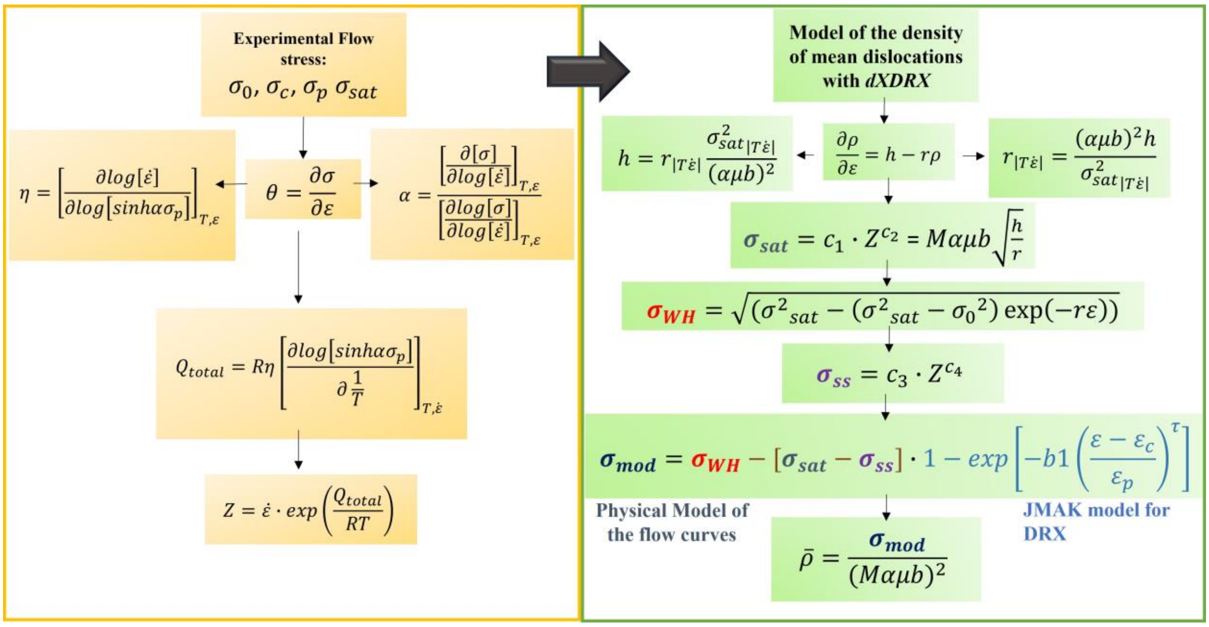

Figure 2. A flowchart was devised to facilitate the mathematical modeling of flow curves and mean dislocation density implementation, considering the fraction of dynamic softening attributed to dynamic recrystallization.

2.1 Wedge-shape forgeability test and numerical modeling

To assess the forgeability of the bainitic steel and explore diverse processing conditions, wedge-shaped geometries were fabricated. This specific geometry (see Figure 3) enables the observation of the effects resulting from varying degrees of strain, strain rate, and temperature within a single specimen. Subsequent to the forging process and water quenching, samples of the austenitic grain size were prepared and subjected to optical microscopy analysis following ASTM E112 standards. Quantification was carried out using the circular intercept method, recommended for materials that may exhibit non-equiaxed grains due to applied deformations, such as those encountered in forging. For visualization of the grain boundaries (AGB), a solution of saturated picric acid containing 42 mL of wetting agent, 58 mL of distilled water, and 2.3 g of picric acid was utilized, with a wetted cotton swab applied to the steel surface for a duration of 5 minutes. To reveal the bainitic microstructure, the samples were etched with a 2% Nital solution by immersion for 10 seconds.

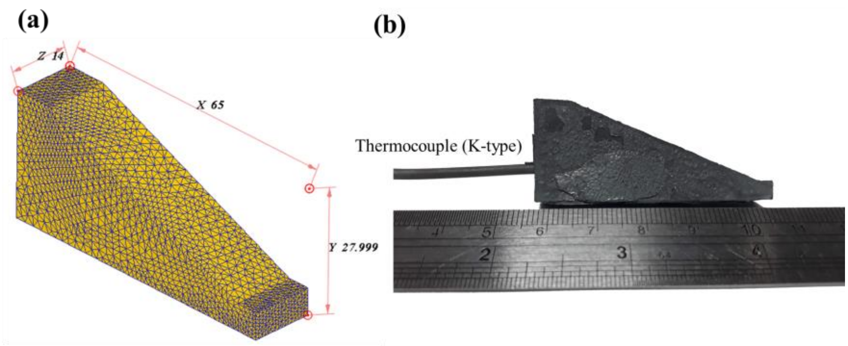

Figure 3. (a) Wedge geometry used to experiment; (b) numerical model.

A coupled simulation of heat transfer and microstructure evolution was carried out using the DEFORM V11.0® rigid-viscoplastic code. The numerical simulation accurately represented the open die forging conditions through a multi-operation code. Tetrahedral elements were utilized to discretize the components within the coupled thermomechanical process. Elastoplastic bodies were incorporated into the upper and lower dies, starting at an initial temperature of 250°C in the forming dies. To address mesh distortion resulting from high plastic strains, the automatic remeshing technique was implemented to effectively model geometry and state variables. Table 1 presents the forging parameters, while Table 2 outlines the boundary conditions established based on forgeability tests.

Table 1. Processing conditions used in the forgeability test.

Forging type	Open die forging
Temperature (°C)	1100
Forming speed (mm/s) / hydraulic press	5
Cooling program	Water quenching/ Continuous cooling
Cooling rate (°C/s)	~ 55/0.5 - 1
Revealing type	Austenite grain boundaries / Bainitic microstructure

The thermal conductivity and heat capacity values for this bainitic steel were obtained from Castro et al., 2021, through inverse heat transfer analysis. A friction factor of 0.3 was employed, indicative of the utilization of graphite and water in the context of open die hot forging.

Table 2. Thermal properties in the numerical model.

Item	Value
Density (g/cm³)	7.83
Heat transfer with pressure considering scale field (N/sec/mm/°C)	11
Air convection coefficient (N/sec/mm/°C)	0.01
Quenching convection coefficient (N/sec/mm/°C)	11

The validation of the microstructure numerical simulation, specifically pertaining to recrystallization and grain growth, is presented in (Ivaniski et al., 2022). The software subroutine was supplemented with all necessary JMAK parameters. The initial austenitic grain size of the wedge-shaped specimen measured 23.5 µm.

2.2 X-ray diffraction experiments for dislocation density determination

After cooling the forged wedges in still air and conducting cross-sectional characterization, the samples underwent electrolytic removal to eliminate the layer with surface-level plastic deformations resulting from prior metallographic preparation. The seventeen regions (R1 - R17) of the piece were subjected to X-ray diffraction analysis and four points were chosen (P1-P4) to compare with numerical results of austenite mean dislocation density, as depicted in Figure 4. The X-ray diffraction parameters were analyzed using the TOPAS software, version 4.2, and Rietveld analysis was performed to calculate the bainite mean dislocation density (ρ_{diff}) as a function of the micro strain (ε) and crystallite size (D) (Rementeria et al., 2017; Smallman; Westmacott; Westucott, 2010) based on equation 1.

$$\rho_{diff} = \frac{3\sqrt{2\pi\varepsilon}}{Db} \tag{1}$$

Where b is the burgers vector.

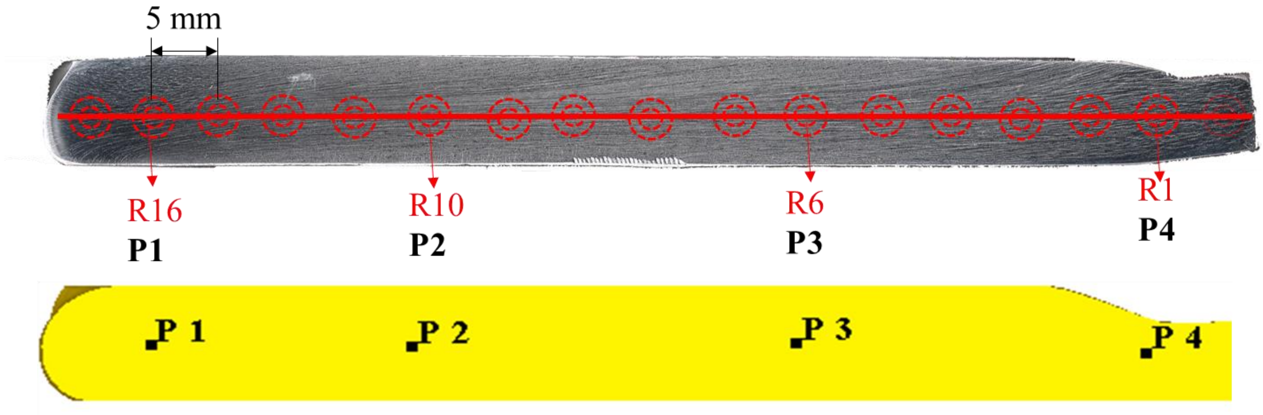

Figure 4. X-ray beam regions of the forged sample and tracked points.

3. RESULTS AND DISCUSSION

3.1 Forgeability effect and microstructure evolution in numerical simulation

Throughout the deformation process, an observable trend emerges wherein an increase in the degree of plastic strain leads to a reduction in temperature due to the heat transfer between the tools and environment (Figure 5b) within the regions highlighted in Figure 5a. In terms of microstructure evolution, the simulation in Figure 5c indicates a more pronounced occurrence of dynamic recrystallization (*XDRX*) in areas with higher effective strain during the process.

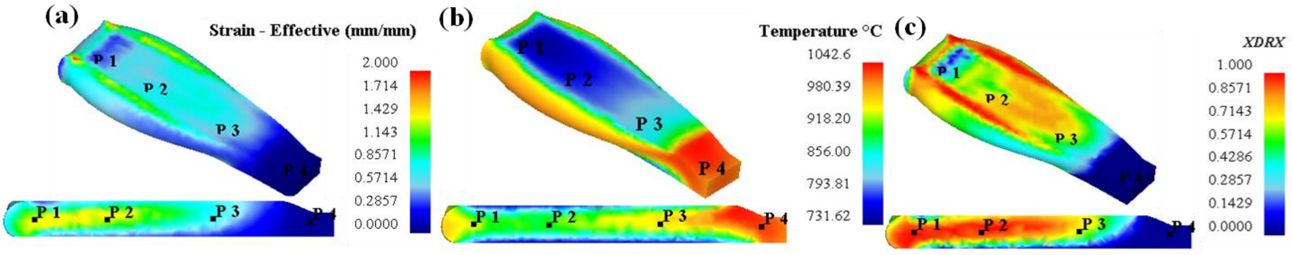

Figure 5. The figure illustrates the Finite Element Analysis (FEA) depicting the and plastic strain (a), temperature evolution (b) and dynamic recrystallized fraction (*XDRX*) (c), in various regions of the wedge workpiece.

In Figure 6, the calculated average austenitic grain size during the processing is showcased and has a good agreement with the experiment. The dominant driving force behind dynamic recrystallization (*XDRX*) in steels lies in the accumulation of energy generated from plastic deformation, surpassing the energy threshold necessary for the nucleation and growth of new grains.

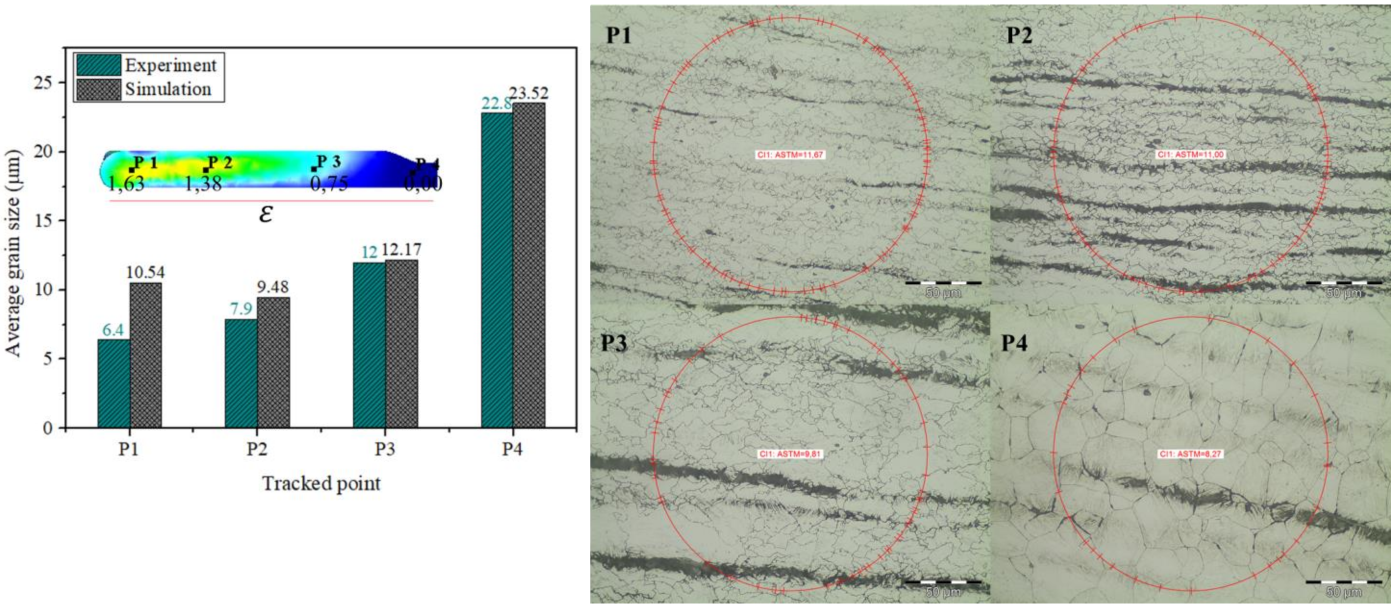

Figure 6. Comparison of experimental and numerical austenitic grain size after forging of the wedges and their respective micrographs.

3.2 Dislocation density analysis

Figure 7 illustrates the dislocation density in the austenitic field during the wedge forging process, while its temporal evolution is depicted in Figure 7b. Evidently, an increase in dislocation density is observed as plastic deformation progresses. Notably, in the specific context of non-isothermal forging, the heat transfer dynamics among the dies, workpiece, and external environment lead to an accelerated cooling rate. Consequently, the dislocation density tends to rise, generating a variation across the part. Moreover, the rate of dynamic recrystallization also exerts influence on the final dislocation density at the end of the process. The timing of the recrystallizing transformation (*XDRX*) at distinct points chosen within the material significantly impacts the equilibrium between dislocation annihilation (nucleation of new grains) and the formation of new dislocations (hardening) in the P1 and P2 regions, relative to the P3 region.

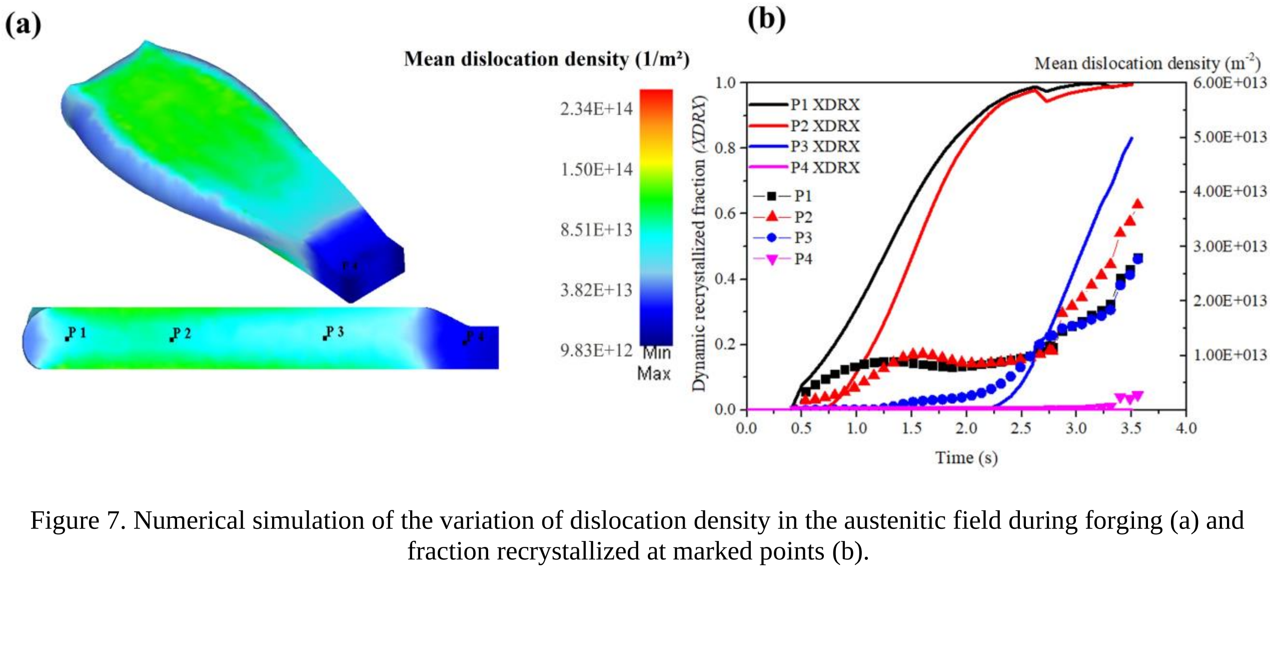

Figure 7. Numerical simulation of the variation of dislocation density in the austenitic field during forging (a) and fraction recrystallized at marked points (b).

This result highlights the importance of analyzing geometric complexity during the thermomechanical processing of hot-forged components. The increase in dislocation density caused by plastic deformation has a significant impact on the resulting dislocation density after phase transformation. Figure 8 illustrates this trend of increasing dislocation quantity after continuous cooling, which justifies, for instance, the enhancement of steel's mechanical strength. However, it is essential to acknowledge certain limitations in these conclusions, such as disregarding the influence of grain boundary orientation, which can lead to specific crystallographic textures. However, it is well known that the grain size affects the final dislocation density, therefore it can be corroborated with the final dislocation density.

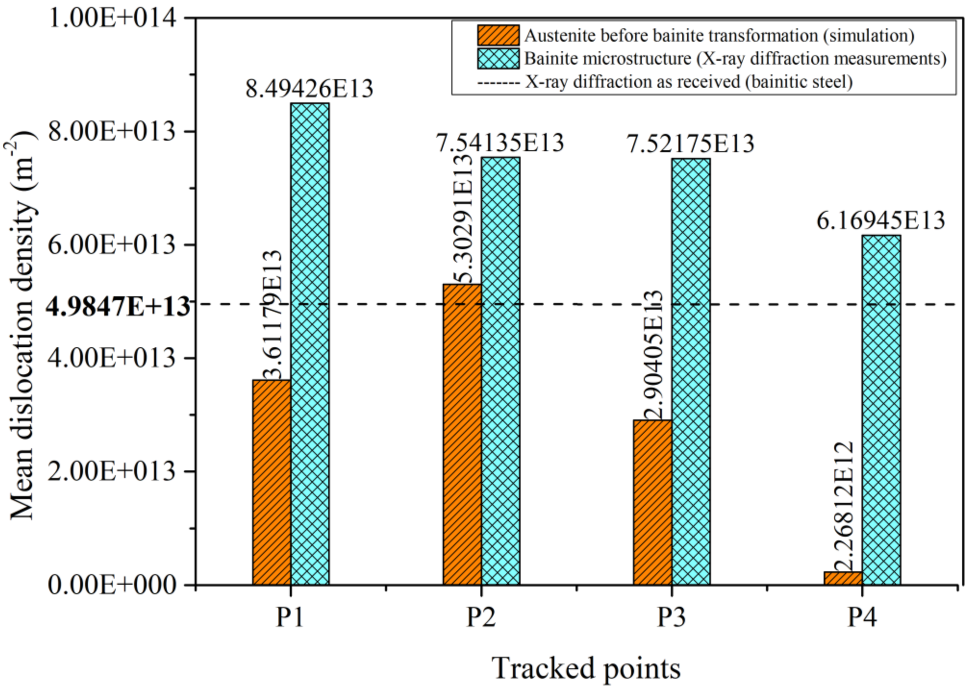

Figure 8. Comparison between the calculation of dislocation density in the austenitic field and after continuous cooling, showing an increasing trend with plastic deformation.

4. CONCLUSION

This research has yielded crucial insights into Continuous Cooling Bainitic Steels and their application in the forging industry:

The results obtained from finite element simulations coupled with X-ray diffraction experiments have provided valuable insights into the relationship between plastic deformation and dislocation density in austenitic field. It has been established that an increase in the degree of plastic strain leads to a proportional rise in dislocation density. This finding corroborates existing knowledge about the role of dislocation density in influencing the kinetics of recrystallization during forging.

Dynamic recrystallization is more pronounced in regions with higher effective strains during forging, influencing the final grain size and dislocation density. The timing and extent of *XDRX* play a crucial role in determining the equilibrium between dislocation annihilation and the formation of new dislocations, ultimately impacting the final dislocation density at the end of the process.

One of the critical takeaways from this study is the importance of considering geometric complexity during the thermomechanical processing of hot-forged components. The increase in dislocation density caused by plastic deformation significantly influences the resulting dislocation density after the continuous cooling bainitic transformation.

Future research should consider grain boundary orientation and explore the effects of varying cooling rates and deformation temperatures. These findings have valuable implications for improving forging processes and achieving superior component properties.

5. ACKNOWLEDGEMENTS

The authors acknowledge the Brazilian agency CAPES (Project 1844/2017) and the Deutsch Forschung gemeinschaft (German Research Foundation – DFG) via project EP 128/6-2 (Project number 327887503) for the financial support within the BRAGECRIM program (Brazilian German Cooperation Research in Manufacturing). To Metal Forming Institute IBF RWTH Aachen in Germany for the support during experimental data acquisition. Thiago M. Ivaniski and Alexandre da S. Rocha also acknowledge CNPq (process numbers 167948/2017-2 and 308773/2018-7) for the grants.

6. REFERENCES

Avrami, M. Kinetics of phase change, I. General theory. J. Chem. Phys. 1939, 7, 1103–1112.

Bhadeshia, H. K. D. H.; Edmonds, D. V. Bainite in silicon steels: new composition–property approach Part 1. Metal Science, [s. l.], v. 17, n. 9, p. 420–425, 1983. Available at: https://doi.org/10.1179/030634583790420646.

Castro PJ, Silveira AC F, Ivaniski TM, Turra CJ, Epp J, Rocha A S. Two-step continuous cooling heat treatment applied in a low carbon bainitic steel. Mater Res. 2021;24(2).

Dalcin, R. L Et Al. Improvement on Pitting Wear Resistance of Gears by Controlled Forging and Plasma Nitriding. Journal of Materials Research and Technology-JMR&T, v. 18, p. 4698-4713, 2022.

Estrin, Y.; Mecking, H. A unified phenomenological description of work hardening and creep based on one-parameter models. Acta Metallurgica, 1984 [s. l.], v. 32, n. 1, p. 57–70.

Hatwig R.A, Dong J, Epp J, Rocha A Da S. Effect of Compressive Deformations on the Final Microstructure of a Low Carbon High Silicon Bainitic Steel Thermomechanically Processed. Mater Res. 2021;24(1):1–7.

Ivaniski T.M, De Souza T, F., Épp J, Rocha A Da S. Constitutive Modelling of High Temperature Flow Behaviour for a Low Carbon High Silicon Bainitic Steel. Mater Res. 2020;23(5).

Ivaniski, T. M. et al. Numerical and experimental study of an industrial case for grain size evolution in bainitic steel in controlled hot forging and its influence on mechanical performance. Materials Research, [s. l.], v. 25, n. 1, 2022.

Ivaniski, T. M.; Epp, Jeremy; Rocha, A. S. Determination of austenitic grain size in hot forming as a function of its variables with the application of subroutines in numerical simulation. In: 41° SENAFOR, 2022, Porto Alegre. 25rd International Forging Conference, 2022. v. 3. p. 77-87.

Jonas JJ, Quelennec X, Jiang L, Martin É. The Avrami kinetics of dynamic recrystallization. Acta Mater. 2009;57(9):2748-56.

Menezes, V. M. Estudo para manufatura energeticamente eficiente de engrenagens através do emprego de aço bainítico de resfriamento contínuo. Master Thesis, Universidade Federal do Rio Grande do Sul, Escola de Engenharia; 2021.

Quelennec, X., Bozzolo, N., Jonas, J. J., & Logé, R. (2011). A new approach to modeling the flow curve of hot deformed austenite. ISIJ International, 51, 945–950

Rementeria, Rosalia Et Al. Quantitative assessment of carbon allocation anomalies in low temperature bainite. Acta Materialia, [s. l.], v. 133, p. 333–345, 2017.

Smallman, R. E.; Westmacott, &. K. H.; Westucott, K. H. Stacking faults in face-centred cubic metals and alloys Stacking Faults in Face-Centred Cubic Metals and Alloyst. [s. l.], n. June 2013, p. 37–41, 2010. Available at: http://www.tandfonline.com/loi/tphm19%5Cnhttp://dx.doi.org/10.1080/14786435708242709%5Cnhttp://www.tandfonline.com/page/terms-and-conditions.

Sourmail, T. Bainite and Superbainite in Long Products and Forged Applications. HTM Journal of Heat Treatment and Materials, [s. l.], v. 72, n. 6, p. 371–378, 2017. Available at: https://doi.org/10.3139/105.110342.

7. RESPONSIBILITY NOTICE

The authors are the only responsible for the printed material included in this paper.